ChemComm

Accepted Manuscript

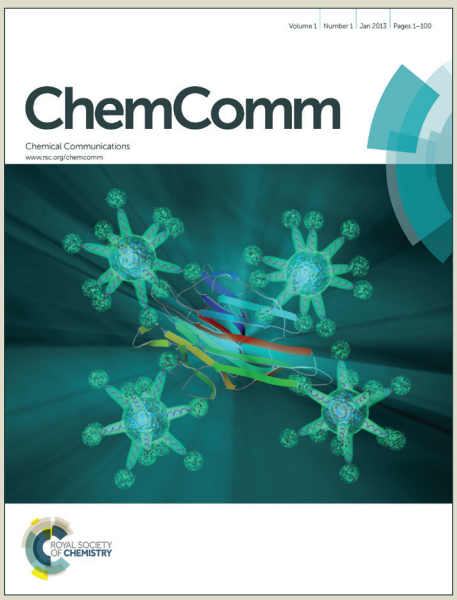

ROYAL SOCIETY OF CHEMISTRY

www.rsc.org/chemcomm

ChemComm

COMMUNICATION

A solution-processed high performance organic solar cells using a small molecule with the thieno[3,2-*b*]thiophene central unit

Received 00th January 20xx,
Accepted 00th January 20xx

DOI: 10.1039/x0xx00000x

www.rsc.org/

Qian Zhang,‡[a] Yunchuang Wang,‡[a] Bin Kan,[a] Xiangjian Wan,*[a] Feng Liu,[b] Wang Ni,[a] Huanran Feng,[a] Thomas P. Russell[b,c] and Yongsheng Chen*[a]

A solution processed acceptor-donor-acceptor (A-D-A) small molecule with thieno[3,2-*b*]thiophene as the central building block and 2-(1,1-dicyanomethylene)-rhodanine as the terminal unit, DRCN8TT,was designed and synthesized. The optimized power conversion efficiency (PCE) of 8.11% was achieved, which is much higher than its analogue molecule DRCN8T. The improved performance was ascribed to the morphology which consisted of small, highly crystalline domains that were nearly commensurate with the exiton diffusion length.

Bulk heterojunction (BHJ) organic photovoltaics (OPVs) have attracted increasing attention due to their advantageous properties, such as lightweight, low-cost, flexibility, and solution-processability.[1] Currently, OPVs are mainly based on two types of electron donor materials, polymers and small molecules. Compared with polymer-based OPVs (P-OPVs), small molecule-based OPVs (SM-OPVs) have some distinct advantages, including a well-defined chemical structure and, therefore, no batch-to-batch variation of the components comprising a device; and versatile chemical structures which enables more facile control over the energy level control.[2] The performance of both polymer-[3]and small molecule-based[4] OPVs (SM-OPVs) are essentially the same, with power conversion efficiencies (PCEs) >10%. The marked improvement of SM-OPVs can be mainly ascribed to the newly designed small molecules and device optimization. Unlike the conventional OPV polymers, where the donor-acceptor structures are incorporated into a single copolymer chain, the molecular design of SM-OPVs imparts tremendous versatility in the design of the fundamental building blocks

In general, the most important building blocks in SM-OPVs are the electron donor aromatic building blocks, such as benzodithiophene (BDT), dithienosilole (DTS), and benzothiadiazole (BT) and etc. New OPV material design reduces to developing a strategy to design, optimize and arrange these aromatic building blocks in the final molecule structures. One such strategy is the fusion of single-ring aromatic blocks. This suppresses intramolecular rotation, enabling good π-electron delocalization along the entire molecule and promotes intermolecular interactions, specifically p-p stacking of the fused rings in the solid state, which improving the light absorption and charge mobility.[5] Thethieno[3,2-*b*]thiophene (TT) block, a fusion of 2,2'-bithiophene,has a stable quinoidal structure, narrow energy band gap, and tendency to exhibit strong intermolecular interactions and packing.[6] Therefore, the TT unit has been extensively used in conjugated polymers for high-performance organic field-effect transistors[7] and OPVs[8]. Yet, TT has been rarely used as a core blocking unit to construct solution processed SM-OPVs with high performance.[9]

We recently reported a series of acceptor-donor-acceptor (A-D-A) oligothiophene based small molecules DRCN4T-DRCN9T, in which the main chains have different thiophene unit numbers from 4 to 9 and the same electron withdrawing end group, 2-(1,1-dicyanomethylene)rhodanine.[4b] Though not fully understood, the devices performances seemed to correlate with the molecular symmetry. Among the DRCN5T–DRCN9T molecules, DRCN5T/7T/9T with odd number of thiophene units gave the best performance, much better than the corresponding DRCN6T/8T. Thus, it would be interesting to design the molecule with the two thiophene units in DRCN8T replaced with one fused TT unit, and examine their OPV performance.

Here, we designed and synthesized a new small molecule **DRCN8TT** using TT as the central unit to replace the two central thiophene units in **DRCN8T**. The new molecule has the same spatial symmetry as **DRCN8T**(Scheme 1). Its photovoltaic performance was systematically investigated and a power conversion efficiency (PCE) of 8.11% was achieved with an optimized thermal annealing treatment under AM 1.5G irradiation (100 mW cm^{-2}), which is much better than **DRCN8T** and very close to the analogue molecules (DRCN7T) having different symmetry[10].The results indicate that significant improvement can be achieved with a minor change on the OPV molecules, highlighting the strong need of a delicate and balanced molecular design to achieve high performance.

[a] *State Key Laboratory and Institute of Elemento-Organic Chemistry and Centre for Nanoscale Science and Technology, Institute of Polymer Chemistry, College of Chemistry, Collaborative Innovation Center of Chemical Science and Engineering (Tianjin), College of Chemistry, Nankai University, Tianjin, 300071, China.*
[b] *Materials Science Divisions, Lawrence Berkeley National Laboratory,Berkeley 94720, United States*
[c] *Polymer Science and Engineering Department, University of Massachusetts, Amherst 01003, United States.*
† Electronic Supplementary Information (ESI) available: [materials, syntheticprocedures, instruments, Figure S1-S11 and Table S1-S5]. See DOI:10.1039/x0xx00000x
‡Q.Z. and Y.C.W contributed equally.

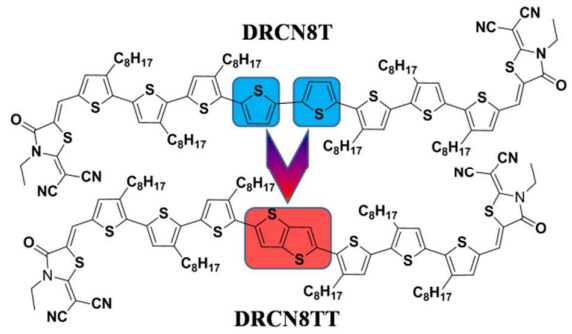

Scheme 1 Chemical structures of **DRCN8T** and **DRCN8TT**.

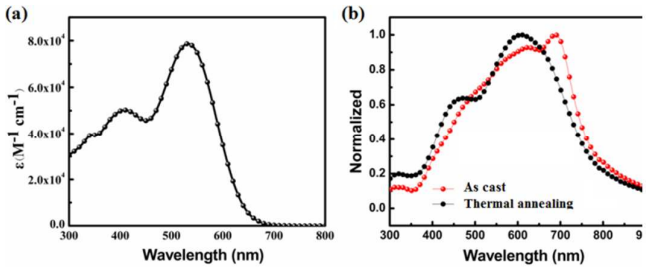

Figure 1 Absorption spectra of **DRCN8TT** in (a) chloroform solution and (b) in films.

The detailed synthetic procedures and the characterization data for **DRCN8TT** are presented in the Electronic Supplementary Information (ESI). The structure of **DRCN8TT** was confirmed by NMR spectroscopy and mass spectrometry. **DRCN8TT** showed good thermal stability with 5% weight loss (T_d) occurring at 395 °C under nitrogen (Figure S1, ESI†), which is comparable to the analogue molecules DRCN5T–DRCN9T.[4b]

The UV-Vis absorption spectra of dilute solutions of **DRCN8TT** in chloroform and in the solid state are shown in Figure 1. In $CHCl_3$ solution, **DRCN8TT** shows an absorption peak at 533 nm and a maximum absorption coefficient of 7.87×10^4 $M^{-1}cm^{-1}$. In the thin film, the spectrum was broadened and obviously red-shifted with a peak at 608 nm. The optical band gap of **DRCN8TT** is estimated to be 1.62 eV. The electrochemical properties of **DRCN8TT** were investigated by cyclic voltammetry (CV) (Figure S2, ESI†). The highest occupied molecular orbital (HOMO) and lowest unoccupied molecular orbital (LUMO) calculated from the onset oxidation and reduction potentials, are -5.08 and -3.46 eV, respectively. The electrochemical band gap of **DRCN8TT** is estimated to be 1.62 eV, consistent with the optical band gap. The absorption and CV data are summarized in Table S1 (ESI†) along with results for **DRCN8T** for comparison. As shown in Table S1, the introduction of TT unit to replace the two thiophene units in **DRCN8T** barely changes its absorption and electrochemical properties. Density functional theory (DFT) calculations at the B3LYP/6-31G(d) level were also used to investigate the electronic structure and geometry of **DRCN8TT** (Figure 2). The optimized geometry for **DRCN8TT** has a centro-symmetric structure. However,

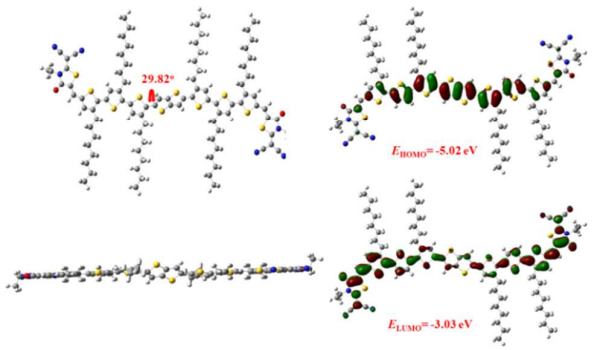

Figure 2 Optimized molecular geometries and frontier molecular orbitals using DFT evaluated at the B3LYP/6-31G(d) level of theory.

unlike that of **DRCN8T** with a nearly planar structure, **DRCN8TT** showed a dihedral angle 29.82° between the TT unit and its adjacent thiophene unit. The indicated dihedral angle might break the great aggregation tendency of fully planar molecules like DRCN8T, thus lead to much different morphology in contrast to that of DRCN8T. Still, the electron density of the HOMO and LUMO extended over the molecular backbone. In addition, the HOMO and LUMO exhibit different patterns of delocalization, e.g., the HOMO is more localized near the central unit of the molecule, while the LUMO is more localized towards the terminal part. This is in contrast to that of **DRCN8T**.

The BHJ solar cells were fabricated using **DRCN8TT** as the electron donor with a conventional device structure of ITO/PEDOT:PSS/**DRCN8TT**:$PC_{71}BM$/PFN/Al (where PFN is poly[(9,9-bis(3'-(N,N-dimethylamino)propyl)-2,7fluorene)-alt-2,7-(9,9–dioctylfluorene)][11]). A range of active layer compositions (**DRCN8TT**:$PC_{71}BM$ weight ratios), film thicknesses, and thermal annealing conditions were systematically investigated. The detailed device fabrication and measurements are described in ESI. Without thermal annealing, the **DRCN8TT**:$PC_{71}BM$ (1:0.8 w/w) devices gave a PCE of 3.65%, with an open circuit voltage (V_{oc}) of 0.90 V, a short circuit current (J_{sc}) of 9.11 mA cm^{-2}, and a fill factor (FF) of 44.6%. After thermal annealing at 130 °C for 10 min, the PCE was sharply improved to 8.11%, with V_{oc}= 0.88 V, J_{sc}= 14.07 mA cm^{-2}, and FF= 65.5%. The current density-voltage(*J-V*) curves of the devices with/without thermal annealing were presented in Figure 3a and the corresponding average photovoltaic parameters are summarized in Table 1. To investigate the effect of thermal annealing on the device performance, UV-Vis absorption spectra of the blend films and the external quantum efficiency (EQE) were measured. As shown in Figure 3b, in comparison with the spectra of as-cast blend film, the spectra of the film with thermal annealing shows a red-shift of 100 nm and shows a nearly flat absorption from 500 to 700 nm with an obvious shoulder peak at 682 nm. As illustrated in the EQE curves (Figure 3c), uniform increases in the spectral response across the wavelength range of 300-800 nm are clearly seen for devices with thermal annealing treatment. The calculated J_{sc} obtained by integration of the EQE curve are 8.77 and 13.47 mA cm^{-2} for the as-cast and optimized devices, respectively, which are within 5% of the J_{sc} values obtained from the *J-V* curves.

For comparison, the photovoltaic parameters of the optimized **DRCN8T** based devices are also summarized in Table 2. From

Table 2, it can be seen that the V_{oc} and FF of the **DRCN8TT** and **DRCN8T** based devices are at the same levels. J_{sc} is the determining factor that leads to the difference of the PCEs, resulting from different morphologies despite of their similar absorption.

Table 1 Photovoltaic parameters for the **DRCN8TT** and **DRCN8T** based optimized devices

Devices	V_{oc} (V)	J_{sc} (mA cm^{-2})	FF	PCE (%)
DRCN8T	0.86	10.80	68.0	6.50(6.37±0.13)
DRCN8TT	0.88	14.07	65.5	8.11(7.91±0.20)

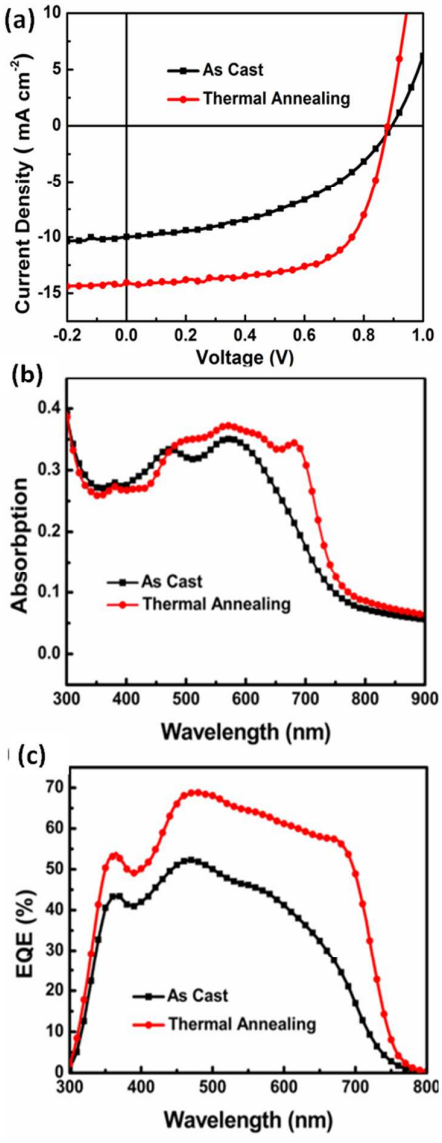

Figure 3 (a) *J-V* curves of **DRCN8TT** based devices with/without thermal annealing; (b) The UV−Vis absorbance spectra of **DRCN8TT**:$PC_{71}BM$ blend with/without thermal annealing; (c) The EQE curves of **DRCN8TT**-based devices with/without thermal annealing.

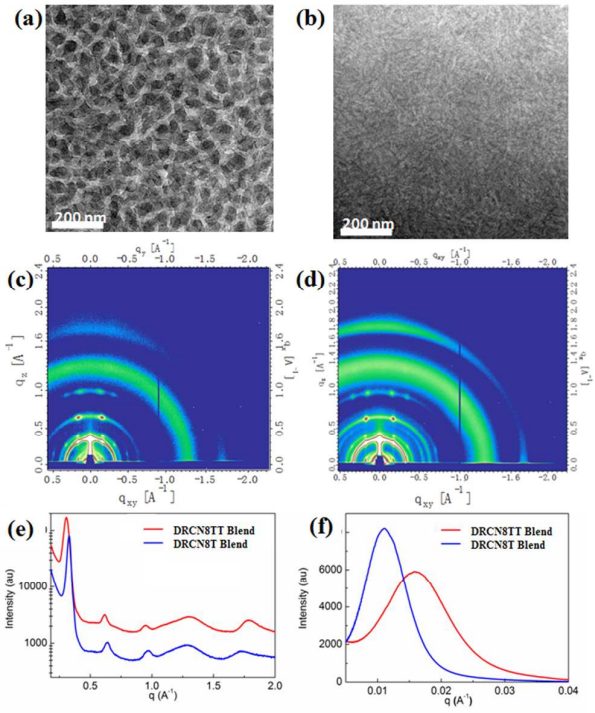

Figure 4 TEM images and GIXD patterns of the active layers: DRCN8T:PC71BM(a, c) and **DRCN8TT**:PC71BM (b, d) under their optimized conditions; Out-of-plane line-cuts of GIXD (e); and R-SoXS (f)of the two molecules based blend films.

To understand the effect of morphology on the photovoltaic performance, we investigated and compared the morphologies of the two small-molecule-based blend films. From atomic force microscopy (AFM) (Figure S6), the surface of both small molecules mixed with PCBM are smooth with a root-mean-square (RMS) roughnesss of 0.81 and 0.53 nm for **DRCN8T** and **DRCN8TT**, respectively. However, there were obvious difference in their transmission electron microscopy (TEM) images (Figure 4a and 4b). **DRCN8TT** showed a better ordered fibrillar structure and smaller domain sizes in comparison to **DRCN8T**, which are nearly commensurate with the exiton diffusion length, i.e.favourable for exciton dissociation. As shown in Figures 4c and 4d, the two-dimensional (2D) grazing-incidence X-ray diffraction (GIXD) patterns for both materials showed multiple, higher order (h00) reflections along q_Z (normal to the film surface), indicating a long-range order and crystallinity in the blend films of both molecules. However, for **DRCN8TT**:$PC_{71}BM$, the lamellar spacing is 18.5 Å (q=0.34 Å) and the π–π stacking distance is 3.53 Å (q= 1.78 Å), which are smaller than those of **DRCN8T** (Table S5). In addition, the full-width half maximum (FWHM) of the (010) reflection (π–π stacking peak) of the **DRCN8TT**:$PC_{71}BM$ film is more obvious and narrower than **DRCN8T**. These results indicate that **DRCN8TT** has stronger molecule interaction and higher crystallinity than **DRCN8T**. These results are also consistent with the blend film mobilities measured by space-charge-limited current (SCLC) method. The optimized **DRCN8TT**-based device gave hole mobility with a value of 6.40× 10^{-4}cm^2 V^{-1} s^{-1}, which is larger than that of the **DRCN8T**-based device (5.77× 10^{-4}cm^2 V^{-1} s^{-1}). To further understand the morphological differences, the resonant soft

X-ray scattering (R-SoXS) of the blend films are shown in Figure3f. **DRCN8TT**:$PC_{71}BM$ blends showed an interference (q= 0.0160 $Å^{-1}$) corresponding to a domain center to center distance of 39 nm, which is smaller than that of **DRCN8T**:$PC_{71}BM$ (q= 0.011 $Å^{-1}$, 57 nm). The values are consistent with the morphology observed by TEM and GIXD. In comparison to **DRCN8T**:$PC_{71}BM$, **DRCN8TT**:$PC_{71}BM$ had a morphology consisting of small highly crystalline domains nearly commensurate with exciton diffusion length, which is favorable for charge transport and improving device performance.[12]

In summary, we have designed and synthesized a new solution-processable A-D-A small molecule donor material **DRCN8TT** by introducing a fused TT unit to replace the two thiophene units in **DRCN8T**. With the same centro-symmetric structure as **DRCN8T**, **DRCN8TT** based devices exhibited a PCE of 8.11 %, which is much higher than that of **DRCN8TT**. The improved performance was attributed to preferred better defined morphology. Taking the results together with that of BDT core based high efficient molecules we have reported[13], which also had the same centro-symmetric structures. these results suggest that there is suitable balance between the molecule structure and packing behavior (morphology). forming and controlling. Thus, it is highly desirable to combine the delicate molecular design and device optimization to strike a suitable balance to achieve highly efficient organic photovoltaic devices.

The authors gratefully acknowledge the financial support from MoST (2014CB643502), NSFC (51373078 , 51422304 and 91433101), PCSIRT (IRT1257) and Tianjin city (13RCGFGX01121) TPR and FL were supported by Polymer-Based Materials for Harvesting Solar Energy (PhaSE), an Energy Frontier Research Center funded by the U.S. Department of Energy, Office of Basic Energy Sciences under award number DE-SC0001087.

Notes and references

1 (a) A. J. Heeger, *Chem. Soc. Rev.*, 2010, **39**, 2354-2371; (b) F. C. Krebs, J. Fyenbo and M. Jørgensen, *J. Mater. Chem*, 2010, **20**, 8994-9001.(c) D. J. Lipomi and Z. Bao, *Energy Environ. Sci.*, 2011, **4**, 3314-3328;(d)F. He and L. Yu, *J. Phys. Chem. Lett.*, 2011, **2**, 3102-3113.

2 (a) B. Walker, C. Kim and T.-Q. Nguyen, *Chem. Mater.*, 2011, **23**, 470-482. (b) J. Roncali, P. Leriche and P. Blanchard, *Adv. Mater.*, 2014, **26**, 3821-3838. (c) Y. Lin, Y. Li and X. Zhan, *Chem. Soc. Rev.*, 2012, **41**, 4245.

3 (a) J. You, L. Dou, K. Yoshimura, T. Kato, K. Ohya, T. Moriarty, K. Emery, C.-C. Chen, J. Gao, G. Li and Y. Yang, *Nat. Commun*, 2013, **4**, No. 1446; (b)J.-D. Chen, C. Cui, Y.-Q. Li, L. Zhou, Q.-D. Ou, C. Li, Y. Li and J.-X. Tang, *Adv. Mater.*, 2015, **27**, 1035-1041.(c) C.-C. Chen, W.-H. Chang, K. Yoshimura, K. Ohya, J. You, J. Gao, Z. Hong and Y. Yang, *Adv. Mater.*, 2014, **26**, 5670-5677.(d) Y. Liu, J. Zhao, Z. Li, C. Mu, W. Ma, H. Hu, K. Jiang, H. Lin, H. Ade and H. Yan, *Nat. Commun*, 2014, **5**. No. 5293.(e) H. Kang, S. Kee, K. Yu, J. Lee, G. Kim, J. Kim, J.-R. Kim, J. Kong and K. Lee, *Adv. Mater.*, 2015, **27**, 1408-1413.(f) Z. He, B. Xiao, F. Liu, H. Wu, Y. Yang, S. Xiao, C. Wang, T. P. Russell and Y. Cao, *Nat. Photonics*, 2015, **9**, 174-179. (g) H. Zhou, Y. Zhang, C. K. Mai, S. D. Collins, G. C. Bazan, T. Q. Nguyen and A. J. Heeger, *Adv. Mater.*, 2015, **27**, 1767-1773. (h)L. Ye, S Zhang, W Zhao, B Yang, Q Wang, J Hou, Sci. China Chem., 2015, **58**, 248-256; (i)C. Liu, C. Yi, K. Wang, Y. Yang, R. S. Bhatta, M. Tsige, S. Xiao and X. Gong, *ACS. Appl. Mater. Interfaces*, 2015, **7**, 4928-4935; (j) S. Liu, P. You, J. Li, J. Li, C.-S. Lee, B. S. Ong, C. Surya and F. Yan, *Energy Environ. Sci.*, 2015, **8**, 1463-1470.

4 (a)Y. Liu, C.-C. Chen, Z. Hong, J. Gao, Y. Yang, H. Zhou, L. Dou, G. Li and Y. Yang, *Sci. Rep,* 2013, **3**. (b) B. Kan, M. Li, Q. Zhang, F. Liu, X. Wan, Y. Wang, W. Ni, G. Long, X. Yang, H. Feng, Y. Zuo, M. Zhang, F. Huang, Y. Cao, T. P. Russell and Y. Chen, *J. Am. Chem. Soc.,* 2015, **137**, 3886-3893.

5 H. Zhou, L. Yang and W. You, *Macromolecules*, 2012, **45**, 607-632.

6 Y.-J. Cheng, S.-H. Yang and C.-S. Hsu, *Chem. Rev.*, 2009, **109**, 5868-5923.

7 (a) I. McCulloch, M. Heeney, C. Bailey, K. Genevicius, I. MacDonald, M. Shkunov, D. Sparrowe, S. Tierney, R. Wagner, W. Zhang, M. L. Chabinyc, R. J. Kline, M. D. McGehee and M. F. Toney, *Nat. Mater*, 2006, **5**, 328-333; (b) H. J. Yun, G. B. Lee, D. S. Chung, Y. H. Kim and S. K. Kwon, *Adv. Mater.*, 2014, **26**, 6612-6616. (c) Z. Fei, P. Patta, Y. Han, B. C. Schroeder, F. Yan, R. J. Kline, T. D. Anthopoulos and M. Heeney, *J. Am. Chem. Soc.*, 2014, **136**, 15154-15157; (d) Y. Li, C.-Y. Chang, Y. Chen, Y. Song, C.-Z. Li, H.-L. Yip, A. K. Y. Jen and C. Li, *J Mater Chem C*, 2013, **1**, 7526-7533.

8 (a)H. Bronstein, Z. Chen, R. S. Ashraf, W. Zhang, J. Du, J. R. Durrant, P. S. Tuladhar, K. Song, S. E. Watkins, Y. Geerts, M. M. Wienk, R. A. Janssen, T. Anthopoulos, H. Sirringhaus, M. Heeney and I. McCulloch, *J. Am. Chem. Soc.*, 2011, **133**, 3272-3275. (b) Y.-X. Xu, C.-C. Chueh, H.-L. Yip, F.-Z. Ding, Y.-X. Li, C.-Z. Li, X. Li, W.-C. Chen and A. K. Y. Jen, *Adv. Mater.*, 2012, **24**, 6356-6361.

9 (a) L. Zhang, F. Liu, Y. Diao, H. S. Marsh, N. S. Colella, A. Jayaraman, T. P. Russell, S. C. Mannsfeld and A. L. Briseno, *J. Am. Chem. Soc.*, 2014, **136**, 18120-18130. (b) D. Deng, S. Shen, J. Zhang, C. He, Z. Zhang and Y. Li, *Org. Electron*, 2012, **13**, 2546-2552.

10 Q. Zhang, B. Kan, F. Liu, G. Long, X. Wan, X. Chen, Y. Zuo, W. Ni, H. Zhang, M. Li, Z. Hu, F. Huang, Y. Cao, Z. Liang, M. Zhang, T. P. Russell and Y. Chen, *Nat. Photonics*, 2015, **9**, 35-41.

11 Z. He, C. Zhong, X. Huang, W.-Y. Wong, H. Wu, L. Chen, S. Su and Y. Cao, *Adv. Mater.*, 2011, **23**, 4636-4643.

12 C. M. Proctor, M. Kuik and T.-Q. Nguyen, *Prog. Polym. Sci*, 2013, **38**, 1941-1960.

13 (a) J. Zhou, Y. Zuo, X. Wan, G. Long, Q. Zhang, W. Ni, Y. Liu, Z. Li, G. He, C. Li, B. Kan, M. Li and Y. Chen, *J. Am. Chem. Soc.*, 2013, **135**, 8484-8487. (b) B. Kan, Q. Zhang, M. Li, X. Wan, W. Ni, G. Long, Y. Wang, X. Yang, H. Feng and Y. Chen, *J. Am. Chem. Soc*., 2014, **136**, 15529-15532. (c)W. Ni, X. Wan, M. Li, Y. Wang and Y. Chen, *Chem. Commun.*, 2015, **51**, 4936-4950.

